# Fluctuation-induced conductivity of polycrystalline $Gd_{1-x}Ce_xBa_2Cu_3O_{7-\delta}$ superconductor

M. Murer, Y. Aparecido Opata, J.F.H. Leandro Monteiro, S. Aparecida da Silva, and P. Rodrigues Júnior
*Departamento de Física, Universidade Estadual de Ponta Grossa,*
*Av. Gen. Carlos Cavalcanti 4748, 84.030-000, Ponta Grossa, Paraná, Brazil.*

A.R. Jurelo
*Departamento de Física, Universidade Estadual de Ponta Grossa,*
*Av. Gen. Carlos Cavalcanti n° 4748, 84.030-000 Ponta Grossa, Paraná, Brazil,*
*Tel : +55 42 3220 3044; Fax : +55 42 3220 3042,*
*e-mail: arjurelo@uepg.br*

Recibido el 2 de mayo de 2012; aceptado el 15 de junio de 2012

This paper reports on measurements of the resistive transition in polycrystalline $Gd_{1-x}Ce_xBa_2Cu_3O_{7-\delta}$ samples ($x = 0.000$, 0.025 and 0.050). The samples were produced by a standard solid state reaction method and in two different thermal routes. The microstructure was analyzed by X-ray diffraction. The samples were considered homogeneous since no extra peaks due to impurity phase were observed. To identify power-law divergences in conductivity, the results were analyzed in terms of the temperature derivative of the resistivity and the logarithmic temperature derivative of the conductivity ($d\ln(\Delta\sigma)/dT$). From the results, the occurrence of a two-stage transition besides the pairing transition splitting for sample with $x = 0.050$ was observed. Such splitting was associated with Ce doping and related with the occurrence of a phase separation. In the normal phase, Gaussian and critical fluctuations conductivity regimes were identified. On approaching the zero resistance state, our results showed a power-law behavior that corresponds to a phase transition from a paracoherent to a coherent state of the granular array.

*Keywords:* High-$T_C$ superconductor; polycrystalline; gadolinium; cerium; critical phenomena; fluctuation effects.

PACS: 74.40.+k; 74.81.Bd; 74.72.-h

## 1. Introduction

The substitution of Y by trivalent rare earth (RE) elements in $YBa_2Cu_3O_{7-\delta}$ (YBCO) yields a superconducting phase with a critical temperature ($T_C$) identical to YBCO [1-2], except for Ce, Tb and Pr. For higher concentrations, Ce and Tb do not replace Y to form a single phase material from the standard solid state reaction technique [3-4], leading to the formation of multiphase samples, with $BaCeO_3$ and $BaCu_2$ always present [5-6]. $PrBa_2Cu_3O_{7-\delta}$ (PBCO) is isostructural to $YBa_2Cu_3O_{7-\delta}$, but is still not superconducting [7]. However, there is also experimental evidence for superconductivity in $PrBa_2Cu_3O_{7-\delta}$. Blackstead *et al.* reported superconductivity in PBCO powders and thin films [8] while Zhou *et al.* have reported bulk superconductivity in single crystals [9].

In the system $Y_{1-x}Pr_xBa_2Cu_3O_{7-\delta}$, $T_C$ decreases monotonically with increasing Pr doping and vanishes at $x \cong 0.56$. In the case of $Y_{1-x}Ce_xBa_2Cu_3O_{7-\delta}$, in a study on thin films, Fincher and Blanchet showed that the partial substitution is possible, with $T_C$ decreasing from 90 K to 55 K for 30 % Ce [10]. It is important to point out that Ce, Pr and Tb have in common the possibility of existing in a tetravalent state, and in that order, are the three rare earth elements most easily ionized to the +4 state [11]. The suppression of $T_C$ with Pr doping for several $RE_{1-x}Pr_xBa_2Cu_3O_{7-\delta}$ compounds has been systematically studied [12-13]. A rare-earth ion size effect on $T_C$ has been observed in these compounds, with $T_C$ decreasing approximately linear when the RE-site ions radius is increased [12-13]. Also, the antiferromagnetic ordering temperature $T_N$ of Pr ions in these compounds decreases monotonically with increasing RE concentration. Gd has a high magnetic moment and as the Pr concentration is increased in $Gd_{1-x}Pr_xBa_2Cu_3O_{7-\delta}$ compound, $T_C$ decreases monotonically, with superconducting state vanishing at a concentration of $x = 0.45$ [14]. For $Gd_{1-x}Ce_xBa_2Cu_3O_{7-\delta}$, Mofakham *et al.* observed in the normal state a metal-insulator transition for $x \cong 0.12$ and the disappearance of the superconducting state for $x \cong 0.6$ [15].

The aim of this work is to carefully study the resistive transition of polycrystalline $Gd_{1-x}Ce_xBa_2Cu_3O_{7-\delta}$ samples ($x = 0.000$, $0.025$ and $0.050$). An important point to study is the influence of the Ce ion in the fluctuation regimes, especially in the critical regimes. The samples were examined by X-ray diffraction and resistivity measurements. The samples were considered homogeneous, since no extra peaks due to impurity phase were observed from the X-ray. The resistivity measurements were analyzed in terms of the temperature derivative of the resistivity ($d\rho/dT$) and also using the logarithmic temperature derivative of the conductivity ($-d\ln(\Delta\sigma)/dT$). The data revealed the occurrence of a two-stage intragranular-intergranular transition besides the pairing transition splitting, which was associated with Ce doping. Near the zero-resistance temperature, a phase transition from a paracoherent to a coherent state of the granular array was observed.

## 2. Experimental Details

Polycrystalline samples of G $d_{1-x}$ C $e_x$ B $a_2$ C $u_3$ $O_{7-\delta}$ ($x = 0.000$, $0.025$ and $0.050$) were prepared by standard solid state reaction technique. Appropriate amounts of $Gd_2O_3$, $Ce_2O_3$, $BaCO_3$ and CuO were mixed and calcinated twice in an alumina crucible at 920°C for 24 h in air. Then, the calcinated powder was pressed into pellets and sintered again at 920° C for 24 h in air. After that, the pellets were slowly cooled to room temperature. Specifically for $Gd_{0.95}Ce_{0.05}Ba_2Cu_3O_{7-\delta}$ concentration, samples were also produced by another thermal treatment. Now, appropriate amounts were mixed, ground and heated at 850 and 880°C in air for 24 hours. Then, they were reground, pressed in pellets and sintered at 920°C for 24 hours and slowly cooled to room temperature. Finally, all the samples were oxygenated under flowing oxygen at 400 $^0$C for 48 h. The room temperature X-ray diffraction patterns were collected using a Rigaku diffractometer with CuK$\alpha$ radiation and $\lambda = 1.542$ Å. Data was collected from 10 to 100° in the $2\theta$ range with 0.02° steps and 4 s counting time. The crystal structure analyses were performed using the GSAS program [16] with the EXPGUI interface [17]. All electrical resistivity measurements were performed from 77 to 300 K by a standard of a four-probe AC technique at the frequency of 37 Hz. The measuring current was limited to 100 mA for bar-shaped samples which were approximately $8\times8\times2$ mm$^2$. The temperature was determined with an accuracy of 0.01 K by precisely measuring the resistance of a Pt-100 sensor.

## 3. Results and Discussion

### 3.1. Characterization

The crystallographic quality of the samples used in this work was checked by x-ray diffraction shown in Fig. 1. The patterns almost completely match the Gd-123 structure (compared with JCPDS files) and belong to the orthorhombic unit cell with symmetry *Pmmm*. Also, they contain no extra peaks, due to impurity phase, within the experimental error. The lattice parameters $a$, $b$, $c$ and V (volume) for $Gd_{1-x}Ce_xBa_2Cu_3O_{7-\delta}$ ($x = 0.00$, $x = 0.025$ and $x$ =0.050) are shown in Table 1. The refinement in room temperature for pure sample gave the following lattice parameters: $a = 3.8528$ (1) Å, $b$ =3.8975 (1) Å, $c = 11.7323$ (1) Å and $V = 176.18$ (1) Å$^3$. Numbers in parentheses are standard deviations of the last significant digits. The values of the lattice parameters $a$ and $c$ decreased to 3.8413 (2) Å and 11.702 (1) Å for $x = 0.05$ sample. On the other hand, $b$ increased to 3.8992 (4) Å for $x = 0.05$ sample. The change of the lattice parameters suggests the presence of Ce inside the grains. Also, the system remains orthorhombic for all $x$ and the lattice constants for $Gd_{1-x}Ce_xBa_2Cu_3O_{7-\delta}$ are consistent with other published results [18]. And finally, the $R_p$ ($R-$pattern), $R_{wp}$ ($R-$weighted pattern) and $\chi^2$ (goodness-of-fit) are compatible with the low count statistics of the measured profile.

TABLE I. Lattice parameters $a$, $b$, $c$ and $V$ for $Gd_{1-x}Ce_xBa_2Cu_3O_{7-\delta}$ ($x = 0.00$, $x = 0.025$ and $x$ =0.050).

| | ***x* = 0.00** | ***x* = 0.025** | ***x* = 0.050** |
|---|---|---|---|
| ***a* (Å)** | 3.8528 (1) | 3.8414 (2) | 3.8413 (2) |
| ***b* (Å)** | 3.8975 (1) | 3.8991(4) | 3.8992 (4) |
| ***c* (Å)** | 11.7323 (1) | 11.703 (1) | 11.702 (1) |
| ***V* (Å$^3$)** | 176.18 (1) | 175.29 (2) | 175.28 (1) |

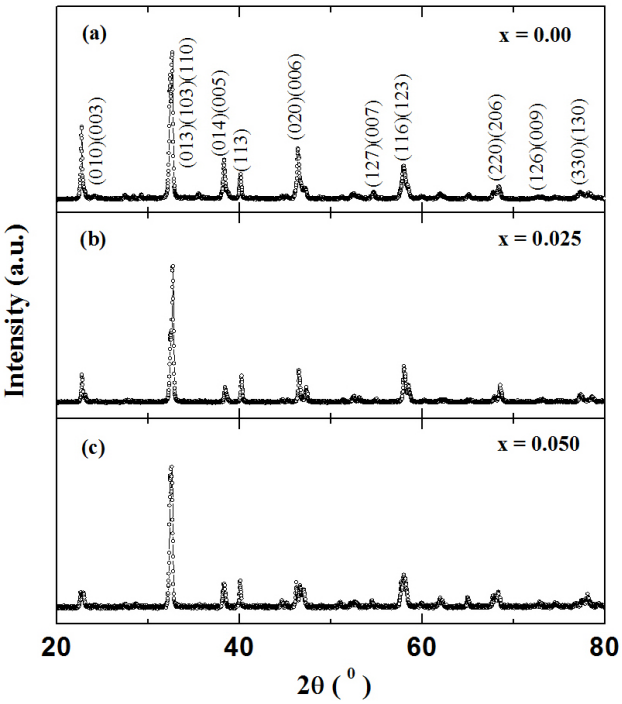


FIGURE 1. Representative X-ray diffraction patterns for (a) $x = 0.00$, (b) $x = 0.025$ and (c) $x$ =0.050 samples.

### 3.2. Method of Analysis

Our method of analysis is based on the numerical determination of the quantity

$$\chi_\sigma \equiv -\frac{d}{dT}\ln(\Delta\sigma), \tag{1}$$

where the fluctuation conductivity is obtained from $\Delta\sigma = \sigma - \sigma_R$. $\sigma(T)$ is the measured conductivity and $\sigma_R(T)$ is the one calculated from extrapolation of high-temperature behavior:

$$\sigma_R = \frac{1}{\rho_R} \tag{2}$$

and

$$\rho_R = \rho_0 + \frac{d\rho_R}{dT}T, \tag{3}$$

where $\rho_0$ and $d\rho_R/dT$ are constants.

Assuming that the fluctuation conductivity diverges as a simple power-law,

$$\Delta\sigma = A\varepsilon^{-\lambda}, \tag{4}$$

where

$$\varepsilon = \frac{(T - T_C)}{T_C}, \tag{5}$$

in analogy with the Kouvel-Fisher method [19] for analyzing critical phenomena, we obtain

$$\chi_\sigma^{-1} = \frac{1}{\lambda}(T - T_C). \tag{6}$$

Thus, the identification of straight lines in plots $\chi_\sigma^{-1}(T)$ allows us to obtain simultaneously the exponent $\lambda$ and critical temperature $T_C$ [20].

### 3.3. Fluctuation Regimes

Measurement of electrical resistivity $\rho(T)$ as a function of temperature for $GdBa_2Cu_3O_{7-\delta}$ sample is displayed in Fig. 2(a). The plot is shown in a narrow temperature range around the critical temperature. The curve is normalized to unity at 100 K and exhibits metallic behavior in the normal state. The measured value for $\rho(T{=}300\text{ K})$ is 5.6 m$\Omega$·cm and is within the range of the reported values for $REBa_2Cu_3O_{7-\delta}$ samples. The transition width, $\Delta T$, defined between 5 % and 95 % of the transition height, is approximately 2 K, and with the zero-resistance temperature around $T_{C0} \cong 90.5$ K.

In Fig. 2(b), a plot of derivative $d\rho/dT$ versus temperature for $GdBa_2Cu_3O_{7-\delta}$ sample is shown. The maximum of $d\rho/dT$, denoted by $T_P$, corresponds approximately to the bulk critical temperature $T_C$ [20]. For Gd-123, $T_P$ is approximately 92.7 K. Around $T_P$, a structure which corresponds to two closely but well resolved maxima can be clearly observed. The temperature splitting, $\Delta \cong 0.5$ K, between the two $d\rho/dT$ peaks, is shown. This kind of structure was also observed in other samples, such as in polycrystalline samples $YBa_2Cu_3O_{7-\delta}$, in single crystal $Bi_2Sr_2Ca_2Cu_3O_{10+x}$ and $Bi_2Sr_2Ca_1Cu_2O_{8+x}$, and also in the simple binary compound $MgB_2$ [21-22]. For $MgB_2$, the splitting was suppressed by applying magnetic fields above 10 kOe parallel to the current orientation [22].

Figure 2(c) shows variations of $\chi_\sigma^{-1}$ against temperature, where the two-stage character of the transition, revealed in this curve by a local minimum around $T_P$ can be observed. Then, the temperature interval relevant for studying fluctuations in the normal phase (above $T_P$) and the regimes dominated by granularity effects (close to the $R = 0$ state) can be identified [23]. We can fit $\chi_\sigma^{-1}$ by three power-law regimes, corresponding to three different exponents. These fits are labeled by the indices $\lambda_{c1}^{(1)}$, $\lambda_{cr}^{(2)}$ (all observed above $T_P$) and $s$ (observed between $T_{C0}$ and $T_P$). Special attention is paid above $T_P$, where critical regimes are observed. Far from $T_P$, the critical exponent $\lambda_{cr}^{(2)} = 0.30 \pm 0.02$ can be observed, which characterizes the asymptotic regime precursor of the pairing transition. The obtained value of 0.30 is consistent with the expectation from the 3D-XY model [24] and was previously observed in several samples of the high-$T_C$ materials, including single crystals, thin films and ceramics [25]. Above $T_P$, the exponent obtained was $\lambda_{cr}^{(1)} = 0.18 \pm 0.02$.

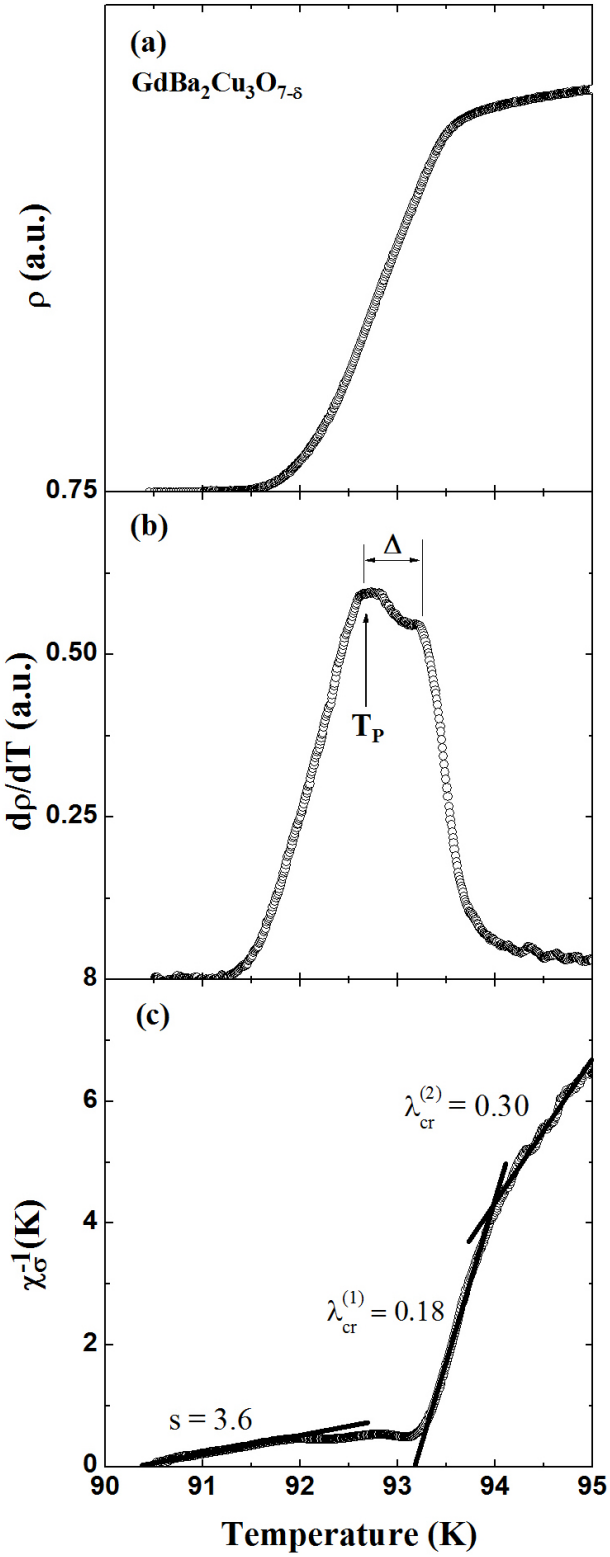


FIGURE 2. Representative results of the resistive transition for a sample of $GdBa_2Cu_3O_{7-\delta}$: (a) resistivity versus temperature, (b) $d\rho/dT$ versus temperature and (c) $\chi_\sigma^{-1}$ versus temperature. $T_P$ is signaled. Straight lines are fits to Eq. (6).

This regime identifies a critical scaling beyond 3D-XY and was first observed by Pureur *et al.*, [26]. Pureur proposed

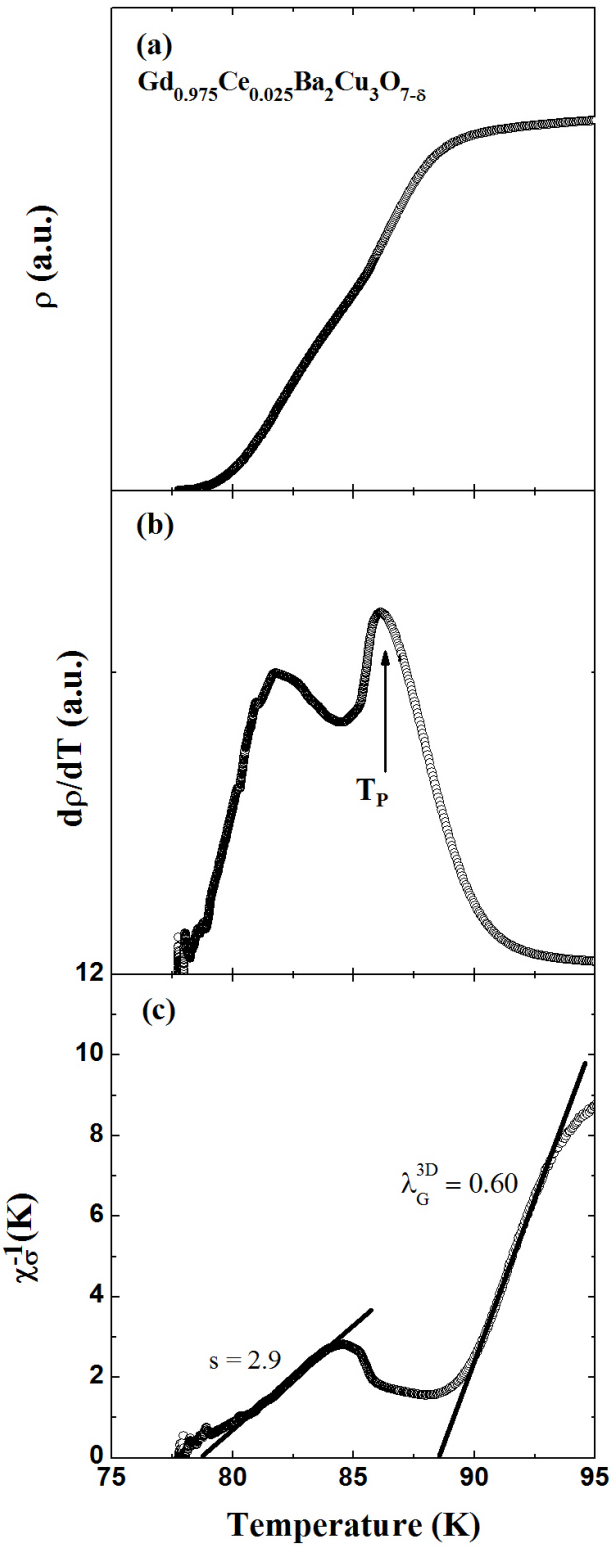


FIGURE 3. Superconducting transition for $Gd_{0.975}Ce_{0.025}Ba_2Cu_3O_{7-\delta}$ sample: (a) resistivity versus temperature, (b) $d\rho/dT$ *versus* $T$ and (c) the inverse of the logarithmic derivative of the conductivity $\chi_\sigma^{-1}$ *versus T*. $T_P$ is signaled.

that this new scaling is associated with a weak first-order transition [26]. Close to the point where the resistivity vanishes, $\chi_\sigma^{-1}$ versus $T$ diverges with exponent $s$=3.6±0.1. This regime is interpreted as being intrinsically related to the superconducting granularity from the mesoscopic/macroscopic level. When the disorder at this level dominates, the fluctuation conductivity near the zero-resistance state must diverge with an exponent $s \cong 3.0$ [27]. The same exponent was also observed in the resistive transition of YBCO ceramics [27].

Figure 3(a) shows the resistivity versus temperature plots for $Gd_{0.975}Ce_{0.025}Ba_2Cu_3O_{7-\delta}$ sample. The current density was 60 mA/cm$^2$ at zero field. The transition width was approximately 10 K and the absolute value of resistivity at room temperature was 2.5 mΩ·cm. Also, the sample showed metallic-like behavior in the normal state (not shown). It can be observed from panel that the critical temperature decreased and that the transition width increased for this small concentration. Figure 3(b) shows $d\rho/dT$ versus $T$. The maximum $d\rho/dT$, denoted by $T_P$, corresponding to the bulk critical temperature can be observed. For the sample with $x = 0.025$, $T_P$ it is approximately 86.2 K. It could also be seen that there is a pronounced peak in the temperature region below $T_P$. A peak or an asymmetry in $d\rho/dT$ occurs systematically in polycrystalline samples [20-23], indicating that the transition is a two-step process. Figure 3(c) shows that above, but close to $T_P$, the variation of $\chi_\sigma^{-1}$ as a function of temperature may be fitted to one straight line. The regime corresponding to the exponent $\lambda_G^{3D} \cong 0.60 \pm 0.02$ is interpreted as resulting from three-dimensional (3D) Gaussian fluctuations. This exponent has been previously reported in $YBa_2Cu_3O_{7-\delta}$ [20], $Bi_2Sr_2CaCu_2O_{8+x}$ (Bi-2212) and $Bi_2Sr_2Ca_2Cu_3O_{10+x}$ (Bi-2223) [23] systems. Between $T_{C0}$ and $T_P$, $\chi_\sigma^{-1}$ is well described by a power law regime, given by the equation $\Delta\sigma \propto (T - T_{C0})^{-s}$, with $s = 2.9 \pm 0.2$. This power-law behavior is suggestive of a phase transition phenomenon and related to the superconducting granularity from the mesoscopic/macroscopic level [27]. The same exponent was also observed in the resistive transition of YBCO ceramics [20].

Figure 4 shows the temperature dependence on the electrical resistivity of $Gd_{0.95}Ce_{0.05}Ba_2Cu_3O_{7-\delta}$ sample at zero external magnetic field. The current density was 60 mA/cm$^2$ at zero field. This sample was heated three times at 920 °C. The measured $\rho(T = 300$ K) is 30 mΩ·cm and is within the range of the reported values for $REBa_2Cu_3O_{7-\delta}$ samples. The figure also shows that the superconducting transition temperature decreased with the increase the Ce doping value, but the transition width remained approximately the same as that for $x = 0.025$, around 12.5 K. In the inset, the temperature dependence of the electrical resistivity of another $Gd_{0.95}Ce_{0.05}Ba_2Cu_3O_{7-\delta}$ sample produced by another thermal treatment to investigate its effect on the splitting of the pairing transition is shown. In this case, the sample was heated at 850 and 880°C and then sintered at 920°C in air for 24 hours. It can clearly seen from the figure that only for the sample heated three times at 920°C the splitting of the pairing transition is present.

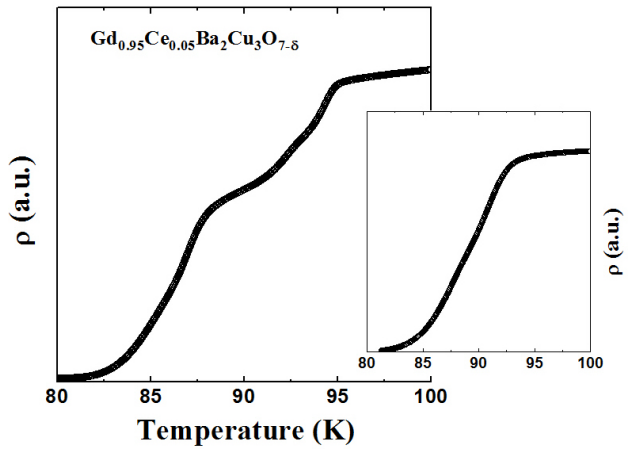


FIGURE 4. Resistivity versus temperature for $Gd_{0.95}Ce_{0.05}Ba_2Cu_3O_{7-\delta}$ sample. Inset: Electrical resistivity $\rho$ as a function of temperature for one sample of $Gd_{0.95}Ce_{0.05}Ba_2Cu_3O_{7-\delta}$ prepared by another thermal route.

Figures 5 and 6 show the resistive transition for polycrystalline $Gd_{0.95}Ce_{0.05}Ba_2Cu_3O_{7-\delta}$ sample. This sample was heated three times at 920 °C. Panels (a) presents $d\rho/dT$ versus temperature plot while panels (b) shows $\chi_\sigma^{-1}$ versus $T$ around the critical temperature. The plot of $d\rho/dT$ versus temperature presents two maxima, denoted by $T_{P1}$ 5(a) and $T_{P2}$ 6(a). Our results indicate clearly that the critical transition splits into two pairing transitions at temperatures $T_{P1}$ and $T_{P2}$. These temperatures correspond approximately to the pairing critical temperatures $T_{C1}$ and $T_{C2}$ [28-30], respectively. The temperature splitting $\Delta = T_{P1} - T_{P2}$ is approximately 7 K. The same splitting of the pairing transition was also observed for other polycrystalline and single crystals Pr- and Ce-doped samples [29-31]. The temperature splitting $\Delta$ does not show changes upon variation of the field and measuring current. Below $T_{P2}$ (panel 6(a)), an asymmetry in $d\rho/dT$ can be observed. A small peak or an asymmetry occurs systematically in polycrystalline samples [20], indicating that the transition is a two-step process [20,27]. The results can be described by an intragrain superconductive transition at $T_{P1}$ (or $T_{P2}$) and an intergrain coherence transition at zero resistance temperature $T_{CO}$ [27].

Figure 5(b) shows $\chi_\sigma^{-1}$ versus $T$ above $T_{P1}$. One regime dominated by Gaussian fluctuations given by exponent $\lambda_G^{3D} \cong 0.49 \pm 0.02$ can be observed. This regime extends by approximately 3 K and corresponds to a regime dominated by 3D Gaussian fluctuations [20]. This result is consistent with those reported for $YBa_2Cu_3O_{7-\delta}$ [20], Bi-2212 [23] and Bi-2223 [23] ceramic samples. Still closer to $T_{P1}$, a critical scaling regime beyond 3D-XY is shown, labeled by the exponent $\lambda_{cr} \cong 0.08 \pm 0.02$. Such regime was first noticed by Costa *et al.* and it was interpreted as revealing an ultimate first-order character of the superconducting transition [26].

Figure 6(b) represents the inverse of the logarithmic derivative of the conductivity for $Gd_{0.95}Ce_{0.05}Ba_2Cu_3O_{7-\delta}$ sample below and above $T_{P2}$. Above $T_{P2}$ the regime dominated by critical fluctuations given by $\lambda_{cr} \cong 0.20 \pm 0.01$ can be observed. As discussed above, this regime beyond $3D - XY$, was first observed by Costa *et al.* in $YBa_2Cu_3O_{7-\delta}$ single crystals and interpreted as a precursor to a weak first-order pairing transition [26]. Between $T_{C0}$ and $T_{P2}$, the variation of $\chi_\sigma^{-1}$ as a function of temperature is better described by a power-law regime given by the equation $\Delta\sigma \sim (T - T_{C0})^{-s}$, with exponent $s = 2.5 \pm 0.2$. This power-law behavior corresponds to a phase transition from a paracoherent to a coherent state of the granular array. The same power-law regime was also observed in the resistive transition in other $REBa_2Cu_3O_{7-\delta}$ ceramics near $T_{C0}$ [27].

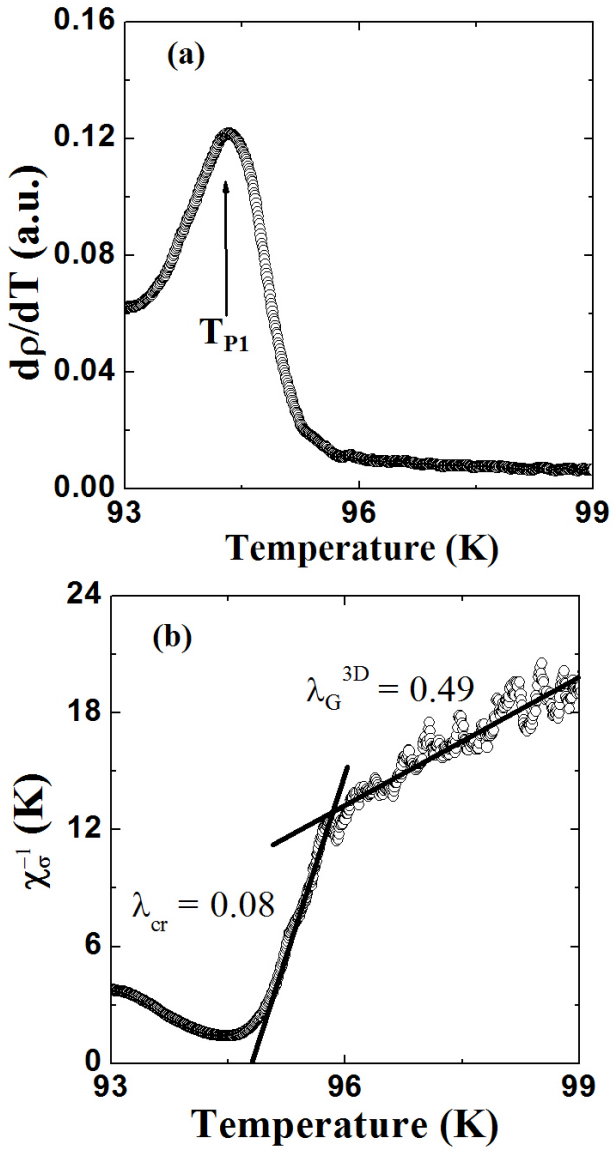


FIGURE 5. (a) $d\rho/dT$ *versus* $T$ and (b) the inverse of the logarithmic derivative of the conductivity $\chi_\sigma^{-1}$ *versus* $T$ for $Gd_{0.95}Ce_{0.05}Ba_2Cu_3O_{7-\delta}$ sample. $T_{P1}$ is signaled.

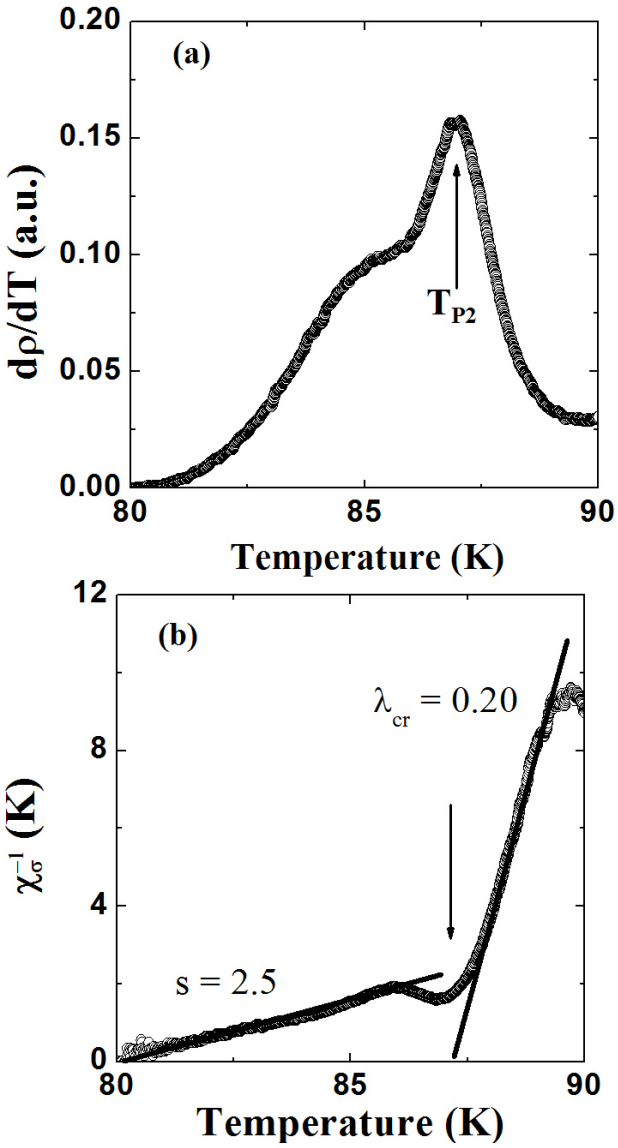


FIGURE 6. (a) $d\rho/dT$ *versus* $T$ and (b) the inverse of the logarithmic derivative of the conductivity $\chi_\sigma^{-1}$ *versus* $T$ for $Gd_{0.95}Ce_{0.05}Ba_2Cu_3O_{7-\delta}$ sample. $T_{P2}$ is signaled.

## 4. Conclusion

In conclusion, our conductivity experiments on granular $Gd_{1-x}Ce_xBa_2Cu_3O_{7-\delta}$ samples ($x = 0.000$, $0.025$ and $0.050$) revealed that the superconducting transition proceeds in two stages: pairing and coherence transition. The results were analyzed in terms of the temperature derivative of the resistivity and of the logarithmic temperature derivative of the conductivity, which allowed identifying power-law divergences in the conductivity. From the analyses, it was clearly observed a pairing transition splitting for sample with $x = 0.050$. Such splitting was associated with Ce doping and related with the occurrence of a phase separation. Close to the zero resistance temperature, a power law regime was found, which suggested the occurrence of a phase transition from a paracoherent to a coherent state of the granular array.

## Acknowledgements

This work was partially financed by the CNPq Brazilian Agency under contract n$^0$ 474077/2007-1.

1. M. B. Maple *et al.*, *Physica B* **148** (1987) 155.
2. S. J. Hagen *et al.*, *Phys. Rev. B* **47** (1993) 1064.
3. K. N. Yang, B. W. Lee, M. B. Maple and S. S. Laderman, *Appl. Phys. A* **46** (1988) 229.
4. L. F. Schneemeyer, J. V. Waszczak, S. M. Zohorak, R. B. Van Dover and T. Siegrist, *Mater. Res. Bull.* **22** (1987) 1467.
5. U. Staub, M. R. Antinio and L. Solderholm, *Phys. Rev. B* **50** (1994) 7085.
6. G. Cao, J. Bolivar, J. W. O'Rielly, J. E. Crow, R. J. Kennedy and P. Pernambuco, *Physica B* **186** (1993) 1004.
7. L. Soderholm *et al.*, *Nature* **328** (1987) 604.
8. H.A. Blackstead *et al.*,*Phys. Rev. B* **54** (1996) 6122.
9. Z. Zou, J. Ye, K. Oka and Y. Nishihara 1998 *Phys. Rev. Lett.* **80** 1074
10. C. R. Fincher and G. B. Blanchet, *Phys. Rev. Lett. B* **67** (1992) 2902.
11. H. A. Blackstead and J. D. Dow, *Phys. Rev. B* **51** (1995) 11830.
12. Y. Xu and W. Guan, *Phys. Rev. B* **45** (1992) 3176.
13. S. K. Malik, C. V. Tomy and P. Bhargava, *Phys. Rev. B* **44** (1991) 7042.
14. Z. Yamani and M. Akhavan, *Solid State Commun.* **107** (1998) 197.

15. S. Mofakham, M. Mazaheri and M. Akhavan, *J. Phys: Condens. Matter.* **20** (2008) 1.
16. A. C. Larson and R. B. Von Dreele, *General Structure Analysis System (GSAS)* (Los Alamos National Laboratory Report LAUR 1994). pp. 86-748.
17. B. H. Toby, *J. Appl. Cryst.* **34** (2001) 210.
18. H. B. Radousky, *J. Matter. Res.* **7** (1992) 1917.
19. J. S. Kouvel and M. E. Fischer, *Phys. Rev.* **136** (1964) A1616.
20. P. Pureur, R. M. Costa, P. Rodrigues Jr., J. Schaf and J. V. Kunzler, *Phys. Rev. B* **47** (1993) 11420.
21. R. M. Costa *et al., Physica C* **251** (1995) 175.
22. F. W. Fabris, R. M. Costa, G. L. F. Fraga, A. S. Pereira, C. A. Perottoni and P. Pureur, *Supercond. Sci. Technol.* **19** (2006) 405.
23. A. R. Jurelo, J. V. Kunzler, J. Schaf, P. Pureur and J. Rosenblatt, *Phys. Rev. B* **56** (1997) 14815.
24. C. Hohenberg and B. I. Halperin, *Rev. Mod. Phys.* **49** (1977) 435.
25. J. Roa-Rojas *et al., Physica C* **341-348** (2000) 1911.
26. R. M. Costa, P. Pureur, M. Gusmão, S. Senoussi and K. Behnia, *Solid State Commun.* **113** (2000) 23.
27. A. R. Jurelo *et al., Physica C* **311** (1999) 133.
28. C. S. Lopes *et al., Mod. Phys. Lett. B* **24** (2010) 1.
29. F. M. Barros *et al., Physica C* **408-410** (2004) 632.
30. F. M. Barros *et al., Phys. Rev. B* **73** (2006) 94.
31. A. R. Jurelo, P. R. Júnior, C. S. Lopes, Y. A. Opata and J. F. H. L. Monteiro, *Supercond. Sci. and Techn.* **25** (2012) 35001.